Available online at www.elixirpublishers.com (Elixir International Journal)

Thermal Engineering

Elixir Thermal Engg. 39 (2011) 4675-4683

ISSN: 2229-712X

Radiation and Dufour effects on chemically reacting MHD mixed convective slip flow in an irregular channel

B. Rushi Kumar and R. Sivaraj

Fluid Dynamics Division, School of Advanced Sciences, VIT University, Vellore – 632 014, India.

ARTICLE INFO

Article history:

Received: 29 July 2011;

Received in revised form: 21 September 2011;

Accepted: 26 September 2011;

Keywords

MHD,
Thermal radiation,
Dufour effect,
Chemical reaction,
Wavy wall.

ABSTRACT

This study examines the problem of MHD mixed convection flow between a horizontal parallel flat wall and a long wavy wall in the presence of thermal radiation, Dufour effect and first order chemical reaction embedded with slip boundary condition. The governing equations include the continuity, linear momentum, energy and mass transfer equations which are solved analytically by using exact solution method. The results of this parametric study on the velocity, temperature and concentration distributions are shown graphically and the physical aspects of the problem are highlighted and discussed. The effect of shear stress, rate of heat and mass transfer coefficients at the channel walls are displayed in tables.

Introduction

Magneto-hydrodynamic equations are ordinary electromagnetic and hydrodynamic equations modified to take into account the interaction between the motion of the fluid and the electromagnetic field. MHD finds applications in electromagnetic pumps, controlled fusion research, crystal growth, plasma jets and chemical synthesis. In view of these applications, (Chamka [1], Umavathi and Malashetty [2], Ahmed and S. Talukdar [3], Mishra et al. [4]) have analyzed the influence of Magnetic field. Mixed convection arises in many natural and technological processes, depending on the forced flow direction. Mixed Convection flows driven by temperature and concentration differences have been studied in the past few decades and find applications in materials processing, dynamics of lakes, crystal growing, float glass production, metal casting, food processing and metal coating. (Baskaya [5], Premachandran and Balaji [6], Chamkha and Ben-Naki [7]) have studied the mixed convection flow to various problems.

The hot walls and the working fluid are usually emitting the thermal radiation within the systems. The role of thermal radiation is of major importance in the design of many advanced energy convection systems operating at high temperature and knowledge of radiative heat transfer becomes very important in nuclear power plants, gas turbines and the various propulsion devices for aircraft, missiles and space vehicles. (Murthy et al. [8], Grosan and Pop [9], Khaefinejad and Aghanajafi [10], Srinivas and Muthuraj [11]) have made investigations of fluid flow with thermal radiation. When the heat and mass transfer occur simultaneously in a moving fluid, the relation between the fluxes and the driving potentials are more intricate in nature. The energy fluxes can also create the concentration gradients and this is the diffusion-thermo or Dufour effect. The Dufour effect is neglected on the basis that it is less significant than the effects described by Fourier and Fick's laws because this effect is considered as second order phenomena. However, this effect is significant in areas such as hydrology, petrology and geo-sciences. We can realize the significance of Dufour effect from the work of (Kafoussias and Williams [12], Anghel et al. [13], Postelnicu [14]).

Convective flow with simultaneous heat and mass transfer under the influence of a magnetic field and chemical reaction have attracted a considerable attention of researchers because such process exist in many branches of science and technology. Chemical reactions can be codified as either heterogeneous or homogeneous processes. This depends on whether they occur at an interface or as a single phase volume reaction. The first order of the chemical reaction is one of the simplest chemical reactions, in which the rate of reaction is directly proportional to the species concentration. The present trend in the field of chemical reaction analysis is to give the mathematical model for the system to predict the reactor performance. The study of chemical reaction is useful in chemical processing industries such as fiber drawing, crystal pulling from the melt and polymer production. The engineering applications include the chemical distillatory processes, formation and dispersion of fog, design of heat exchangers, channel type solar energy collectors and thermo-protection systems. In view of these applications, (Kandasamy and Anjali Devi [15], Kandasamy et al. [16], Seddeek [17],

Mansour et al. [18]) have examined the effect of chemical reaction. The fluid exhibits non-continuum effects such as slip flow when the molecular mean free-path length of the fluid is comparable to the distance between the walls. The knowledge of flows with slip boundary condition would be more useful for chemical engineering fields, for example flow through pipes in which chemical reaction occurs at the walls.

Tele:
E-mail addresses: rushikumar@vit.ac.in ,Sivaraj.kpm@gmail.com

(Joshi and Denn [19], Ebaid [20], Makinde and Chinyok [21], Rushi Kumar and Sivaraj [22]) have investigated the effectiveness of slip boundary condition. Previous studies of the flows of heat and mass transfer have focused mainly on a flat wall or a regular channel. It is necessary to study the heat and mass transfer in an irregular channel because irregular channels are present in many applications. The study of viscous flows bounded by wavy wall is more interest due to its application in transpiration cooling of re-entry vehicles, rocket booster, cross-hatching on ablative surfaces and film vaporization in combustion chambers. (Cho et al. [23], Tashtoush and Al-Odat [24], Hady et al. [25]) have analyzed the effect of fluid flow in wavy channels. Muthuraj and Srinivas [26] studied the effect of fluid flow between parallel flat wall and a long wavy wall in a horizontal channel.

To the best of our knowledge, the influence of thermal radiation and chemical reaction in MHD mixed convective boundary layer slip flow between parallel flat wall and a long wavy wall has not been studied before. Therefore the main goal here is to construct a mathematical model to understand the effect of flow, heat and mass transfer on chemically reacting MHD flow of a Newtonian fluid in a two dimensional irregular channel, in the presence of temperature dependent heat source, absorption of radiation and Dufour effect. The features of the flow and heat and mass transfer characteristics are analyzed by plotting graphs and discussed in detail. The following procedure is adopted in the rest of the paper. In Section 2, the problem is formulated. Section 3 includes the analytic solutions for the problem. Section 4 contains numerical results and discussion. The conclusions are summarized in Section 5.

Formulation of the problem

Consider the steady, two-dimensional, horizontal flow of an electrically conducting viscous incompressible fluid flow between parallel wall and a long wavy wall subject to slip boundary condition at the interface of fluid layers. The $x-$axis is taken along the wall in horizontal direction and the $y-$axis is taken normal to it. The flat wall $y=0$ maintains a constant temperature T_1 and concentration C_1, lower than the wavy wall $y=d+\varepsilon^* \cos kx$ which maintains temperature T_2 and concentration C_2 respectively. The governing equations for this investigation are based on the balance laws of mass, linear momentum, energy and concentration have modified into take the account of transverse magnetic field, buoyancy, thermal radiation, heat source, absorption of radiation, Dufour effect and chemical reaction. Rests of the fluid properties are assumed to be constant. These can be written in Cartesian coordinates as follows:

$$\frac{\partial u}{\partial x}+\frac{\partial v}{\partial y}=0 \tag{1}$$

$$\left(u\frac{\partial u}{\partial x}+v\frac{\partial u}{\partial y}\right)=-\frac{1}{\rho}\frac{\partial p}{\partial x}+\nu\left(\frac{\partial^2 u}{\partial x^2}+\frac{\partial^2 u}{\partial y^2}\right)- \frac{\sigma B_0^2}{\rho}u+g\beta_T\left(T-T_1\right)+g\beta_C\left(C-C_1\right) \tag{2}$$

$$\left(u\frac{\partial T}{\partial x}+v\frac{\partial T}{\partial y}\right)=\frac{K}{\rho C_p}\left(\frac{\partial^2 T}{\partial x^2}+\frac{\partial^2 T}{\partial y^2}\right)- \frac{1}{\rho C_p}\left(\frac{\partial q_r}{\partial x}+\frac{\partial q_r}{\partial y}\right)-\frac{Q_T\left(T-T_1\right)}{\rho C_p}+ \frac{Q_C\left(C-C_1\right)}{\rho C_p}+\frac{D_m K_T}{\rho C_S C_p^2}\left(\frac{\partial^2 C}{\partial x^2}+\frac{\partial^2 C}{\partial y^2}\right) \tag{3}$$

$$\left(u\frac{\partial C}{\partial x}+v\frac{\partial C}{\partial y}\right)=D_m\left(\frac{\partial^2 C}{\partial x^2}+\frac{\partial^2 C}{\partial y^2}\right)- K_l\left(C-C_1\right) \tag{4}$$

The appropriate boundary conditions for velocity, temperature and concentration fields are

$$u=L_1\left(\frac{\partial u}{\partial y}\right),\ v=-V_0,\ T=T_1,\quad C=C_1\quad at\quad y=0 \tag{5}$$

$$u=-L_1\left(\frac{\delta u}{\delta y}\right),\ v=0,\ T=T_2,\quad C=C_2\quad at\quad y=d+\varepsilon^*\cos kx \tag{6}$$

Since the flat wall is infinite in length, therefore

$$\frac{\partial u}{\partial x}=0 \tag{7}$$

The radiative heat flux is given by Cogley et al. [27] as

$$\frac{\partial q_r}{\partial y}=4\left(T-T_1\right)I' \tag{8}$$

Integrate equation (1) and use equation (5), we obtain

$$v=-V_0 \tag{9}$$

We introduce the following non-dimensional variables

$$\left(X,Y\right)=\frac{1}{d}\left(x,y\right),\ \left(U,V\right)=\left(\frac{u}{U_0},\frac{v}{V_0}\right),\quad P=\frac{pd}{\mu V_0},\ \ \theta=\frac{T-T_1}{T_2-T_1},\ \ \phi=\frac{C-C_1}{C_2-C_1} \tag{10}$$

In view of equations (7)-(10), the governing equations (2)-(4) yield

$$\frac{d^2U}{dY^2}+R\frac{dU}{dY}-M^2U+\frac{Gr}{Re}\theta+\frac{Gc}{Re}\phi+A=0 \tag{11}$$

$$\frac{d^2\theta}{dY^2}+PrR\frac{d\theta}{dY}-\left(F+\alpha_T\right)\theta+ \alpha_C\phi+Df\frac{d^2\phi}{dY^2}=0 \tag{12}$$

$$\frac{d^2\phi}{dY^2}+Pe\frac{d\phi}{dY}-K_L\phi=0 \tag{13}$$

The appropriate boundary conditions become

$$U = \gamma U',\ \ V = -1,\ \ \theta = 0,\quad \phi = 0 \quad at \quad Y = 0 \qquad (14)$$

$$U = -\gamma U',\ V = 0,\ \theta = 1,\quad \phi = 1 \ \ at \ \ Y = h \qquad (15)$$

Solution of the problem

The solution for fluid velocity, temperature and concentration are obtained from the equations (11)-(15) as follows:

$$U(Y) = A_7 e^{\beta_1 y} + A_8 e^{\beta_2 y} + A_9 e^{\beta_3 y} + A_{10} e^{\beta_4 y} + A_{11} + A_{12} e^{\beta_5 y} + A_{13} e^{\beta_6 y} \qquad (16)$$

$$\theta(Y) = A_3 e^{\beta_1 y} + A_4 e^{\beta_2 y} + A_5 e^{\beta_3 y} + A_6 e^{\beta_4 y} \qquad (17)$$

$$\phi(Y) = A_1 e^{\beta_1 y} + A_2 e^{\beta_2 y} \qquad (18)$$

The shear stress, the coefficient of the rate of heat transfer and the rate of mass transfer at any point in the fluid can be characterized by

$$\tau^* = -\mu u' ;\ Nu^* = -kT' ;\ Sh^* = -DC' \qquad (19)$$

In dimensionless form

$$\tau = \frac{\tau^* d}{\mu U_0} = -U' ;\ Nu = \left(\frac{Nu^* d}{k(T_1 - T_0)}\right) = -\theta' ;$$

$$Sh = \left(\frac{Sh^* d}{C_1 - C_0}\right) = -\phi' \qquad (20)$$

The skin friction (τ), the Nusselt number (Nu) and the Sherwood number (Sh) at the flat wall $Y = 0$ and the wavy wall $Y = h$ are given by

$$\tau_0 = U'\big|_{Y=0} = A_7\beta_1 + A_8\beta_2 + A_9\beta_3 + A_{10}\beta_4 + A_{12}\beta_5 + A_{13}\beta_6 \qquad (21)$$

$$\tau_1 = U'\big|_{Y=h} = A_7\beta_1 e^{\beta_1 h} + A_8\beta_2 e^{\beta_2 h} + A_9\beta_3 e^{\beta_3 h} + A_{10}\beta_4 e^{\beta_4 h} + A_{12}\beta_5 e^{\beta_5 h} + A_{13}\beta_6 e^{\beta_6 h} \qquad (22)$$

$$Nu_0 = -\theta'\big|_{Y=0} = -\begin{pmatrix} A_3\beta_1 + A_4\beta_2 + \\ A_5\beta_3 + A_6\beta_4 \end{pmatrix} \qquad (23)$$

$$Nu_1 = -\theta'\big|_{Y=h} = -\begin{pmatrix} A_3\beta_1 e^{\beta_1 h} + A_4\beta_2 e^{\beta_2 h} + \\ A_5\beta_3 e^{\beta_3 h} + A_6\beta_4 e^{\beta_4 h} \end{pmatrix} \qquad (24)$$

$$Sh_0 = -\phi'\big|_{Y=0} = -\left(A_1\beta_1 + A_2\beta_2\right) \qquad (25)$$

$$Sh_1 = -\phi'\big|_{Y=h} = -\left(A_1\beta_1 e^{\beta_1 h} + A_2\beta_2 e^{\beta_2 h}\right) \qquad (26)$$

where the primes denote the derivative with respect to Y.

Result and Discussion

This section provides the behavior of parameters involved in the expressions of flow, heat and mass transfer characteristics. The graphical representation of results is very useful to discuss the physical features presented by the solutions. Throughout the computations we employ $A = 0.5$, $R = 0.5$, $M = 2$, $Gr = 4$, $Gc = 2$, $\text{Re} = 1$, $\gamma = 0.02$, $Pr = 2$, $F = 1$, $Df = 1$, $\alpha_T = 2$, $\alpha_C = 2$, $Pe = 1$, $K_L = 1$, $\varepsilon = 0.002$ and $X = 1$ unless otherwise stated.

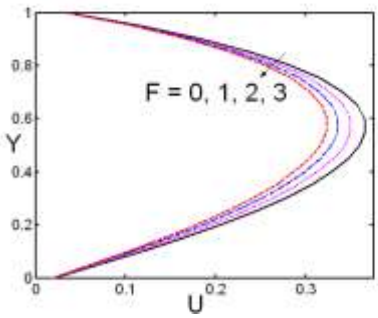

Figure 1: Effect of radiation parameter in velocity distribution

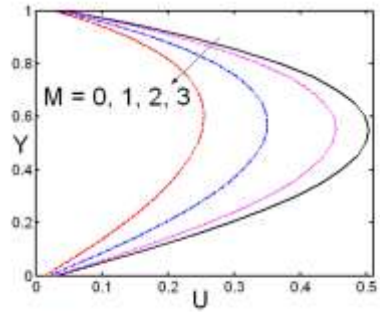

Figure 2: Effect of magnetic field in velocity distribution

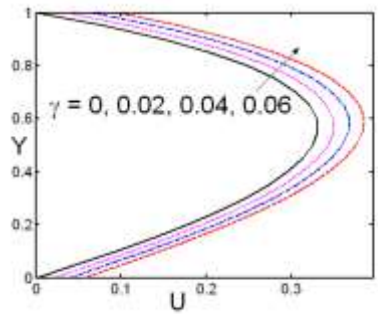

Figure 3: Effect of slip parameter in velocity distribution

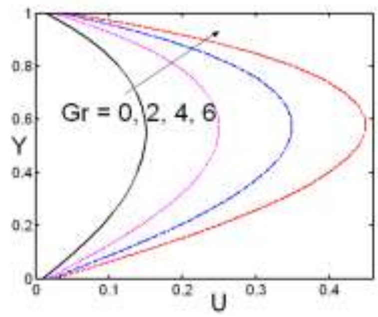

Figure 4: Effect of thermal Grashof number in velocity distribution

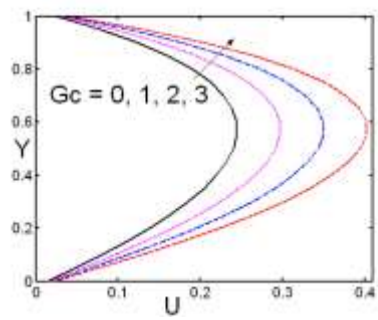

Figure 5: Effect of solutal Grashof number in velocity distribution

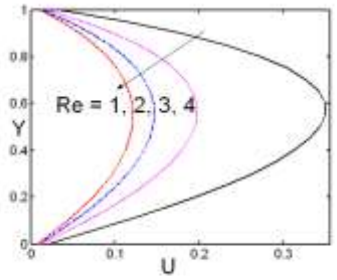

Figure 6: Effect Reynolds number in velocity distribution

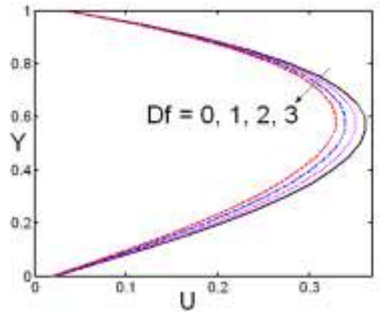

Figure 7: Effect of Dufour number in velocity distribution

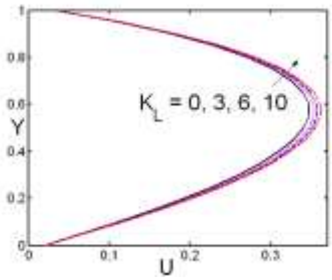

Figure 8: Effect of chemical reaction parameter in velocity distribution

Figure 1 elucidates that the increase in the radiation parameter decreases the fluid velocity. The effect of magnetic field on velocity profiles is graphed in Fig. 2.

Increase in magnetic field monotonically decreases the fluid velocity throughout the boundary layer because it gives rise to a resistive force called the Lorentz force which acts opposite to the flow direction. It is clear from Fig. 3 that the increase in slip parameter leads to enhance the velocity because it reduces the friction force.

Figures 4 and 5 represent the influence of the thermal and solutal buoyancy forces respectively. Increases in these forces significantly increase the boundary layer thickness which resulted into rapid enhancement of fluid velocity. Figures 6 and 7 illustrate that the velocity profiles decrease for increasing Reynolds number and Dufour effect.

Increases in the chemical reaction parameter increase the fluid velocity and the curves could be seen in Fig. 8.

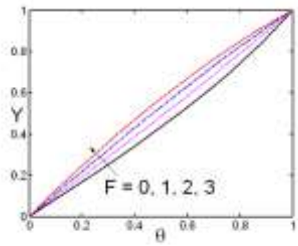

Figure 9: Effect of radiation parameter in temperature distribution

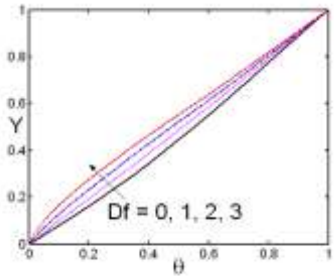

Figure 10: Effect of Dufour number in temperature distribution

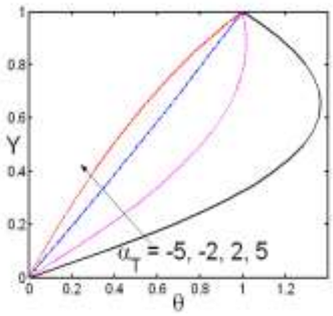

Figure 11: Effect of heat source parameter in temperature distribution

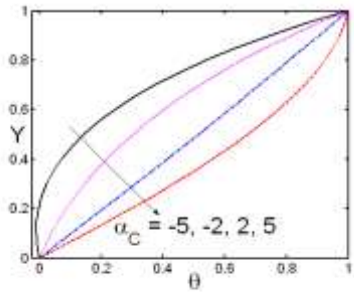

Figure 12: Effect of radiation absorption parameter in temperature distribution

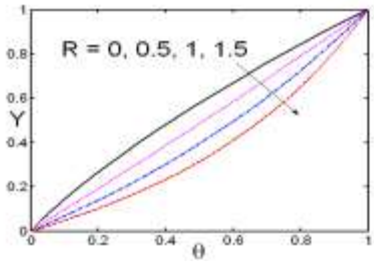

Figure 13: Effect of suction parameter in temperature distribution

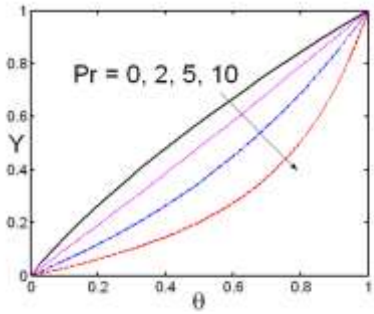

Figure 14: Effect of Prandtl number in temperature distribution

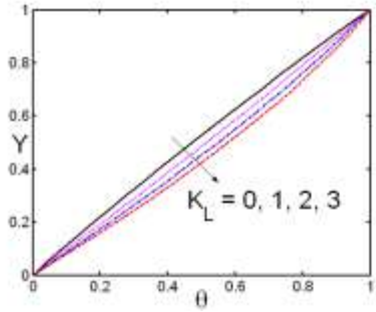

Figure 15: Effect of chemical reaction parameter in temperature distribution

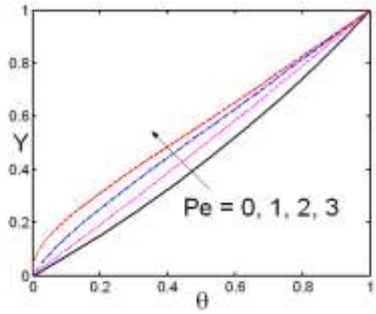

Figure 16: Effect of Peclet number in temperature distribution

Figure 9 represents that increase in the radiation parameter increases the temperature distribution because large values of radiation parameter oppose the conduction over radiation, thereby which increases the thickness of the thermal boundary layer. Figure 10 shows that increase in Dufour number significantly increase the thermal boundary layer thickness which increases the fluid temperature. The heat source parameter has tendency to increase the thermal buoyancy effects which raise the fluid temperature and it is plotted in Fig. 11. Figure 12 illustrates that the radiation absorption parameter decreases the heat transfer because it observes the thermal radiation and so the fluid temperature falls. The fluid temperature decreases for increasing suction which is displayed in Fig. 13. Figure 14 presents that the increase in Prandtl number raises the thermal conductivities and therefore heat is able to diffuse away from the heated channel and the fluid temperature is reduced. The increments in the chemical reaction parameter result in decrease the boundary layer thickness and reduce the heat transfer which is graphed in Fig. 15. Heat transfer of the fluid significantly increases for increasing the Peclet number and it is displayed in Fig. 16.

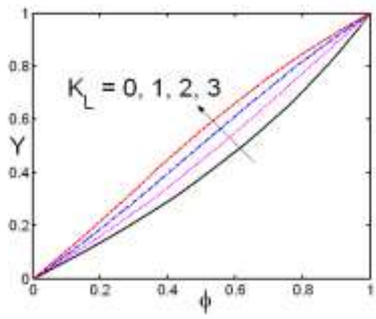

Figure 17: Effect of chemical reaction parameter in concentration distribution

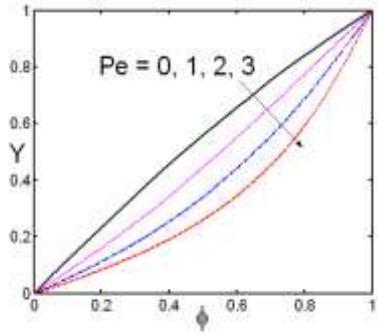

Figure 18: Effect of Peclet number in concentration distribution

It is observed from the Fig. 17 that we obtain a constructive type chemical reaction because the concentration increases for increasing the chemical reaction parameter which indicates that the diffusion rates can be changed by the chemical reaction. Figure 18 illustrates that increases in Peclet number increase the conduction which decrease the mass transfer.

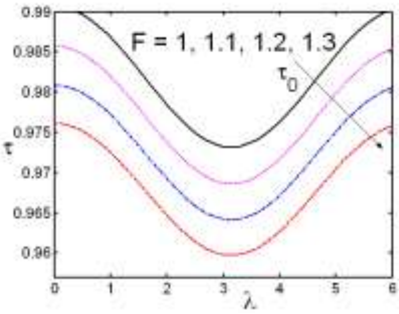

Figure 19: Effect of radiation parameter in skin friction distribution at the flat wall

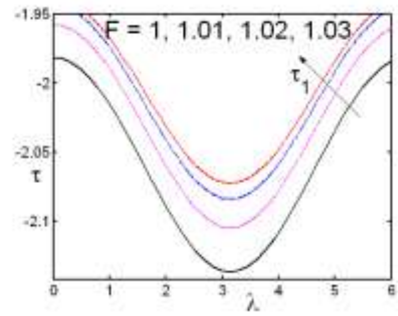

Figure 20: Effect of radiation parameter in skin friction distribution at the wavy wall

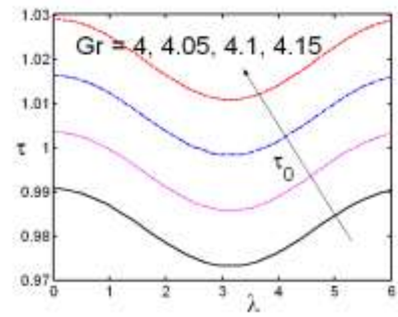

Figure 21: Effect of thermal Grashof number in skin friction distribution at the flat wall

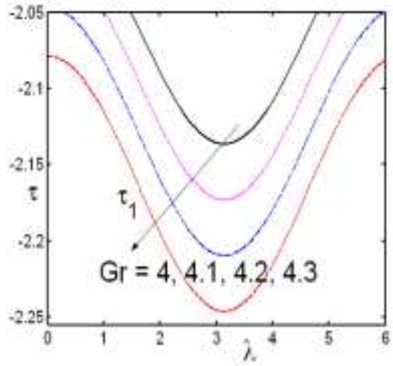

Figure 22: Effect of thermal Grashof number in skin friction distribution at the wavy wall

Figures 19-22 illustrates the effects of F and Gr on the skin friction against frequency parameter. The magnitude of skin friction decreases with an increase of radiation parameter at the flat wall $Y = 0$ which is displayed in Fig. 19 but this trend is reversed at the wavy wall $Y = h$ which is shown in Fig. 20. Figure 21 elucidates that the shear stress increases at the flat wall for increasing thermal Grashof number while it decreases at the other wall which is displayed in Fig. 22.

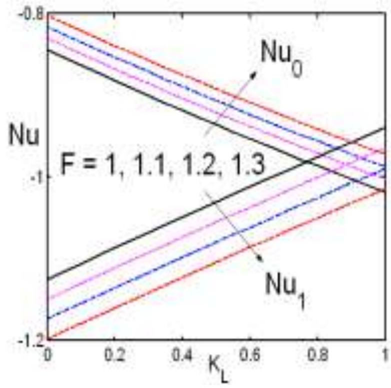

Figure 23: Effect of radiation parameter in Nusselt number distribution

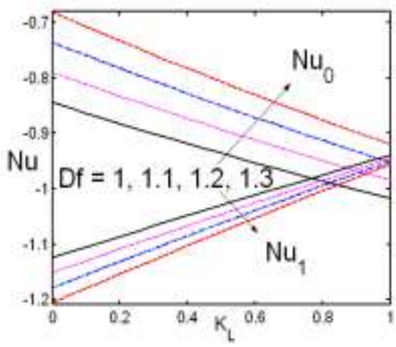

Figure 24: Effect of Dufour number in Nusselt number distribution

The effect of F and Df on Nusselt number distribution with respect to chemical reaction parameter is plotted in Figs. 23 and 24. Nusselt number increases with an increase of radiation parameter at the flat wall $Y = 0$ but this behavior is reversed at the wavy wall $Y = h$ and this is depicted in Fig. 23. Figure 24 shows that the Nusselt number distribution increases for increasing Dufour number at the flat wall but the reverse trend is obtained at the wavy wall.

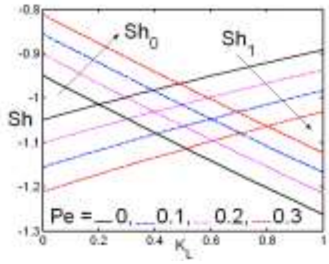

Figure 25: Effect of Peclet number in Sherwood number distribution

Figure 25 shows the effect of Sherwood number distribution (Sh) with respect to chemical reaction parameter. Sherwood number increases for increasing Peclet number at the flat wall but it produces the reverse effect at the wavy wall. It is observed that the agreement of all profiles with the theoretical solution is excellent.

Table 1 is presented to show the influence of F, α_T, α_C and Df thermal radiation parameters, heat absorption parameter, radiation absorption parameter and Dufour effect in skin friction and Nusselt number at the walls. Table 2 represents the effect of chemical reaction parameter, Peclet number and frequency parameter in skin friction, Nusselt number and Sherwood number at the walls.

Conclusions

We have analyzed the steady MHD mixed convective boundary layer slip flow in an irregular channel with the influence of thermal radiation, Dufour effect and chemical reaction. The effects of various significant parameters entering into the problem have been discussed with graphical illustrations. We notice the following key observations from this study. Increase in the magnetic field increase the Lorentz force which decreases the fluid velocity. The raise in Reynolds number, thermal radiation and Dufour effects are having the tendency to decrease the buoyancy effect and diminish the fluid velocity whereas increase in slip parameter and chemical reaction increase the fluid velocity. The increase in thermal radiation, heat source parameter, Dufour effect as well as Peclet number raises the temperature because they increase the boundary layer thickness and the heat is not able to diffuse away but the radiation absorption parameter, suction parameter, Prandtl number and chemical reaction reverse the trend. The fluid concentration decreases for increasing chemical reaction parameter but the Peclet number reverses the effect. Furthermore it is clear from this examination that the Dufour effect should be consider as well for the fluids with light molecular weight.

References

[1] Chamka AJ. MHD flow of a uniformly stretched vertical permeable surface in the presence of heat generation/ absorption and a chemical reaction. Int. Comm. Heat Mass Transfer. 2003; 30: 413–22.

[2] Umavathi JC, Malashetty MS. Magnetohydrodynamic mixed convection in a vertical channel. Int. J. Non-linear Mech. 2005; 40; 91–101.

[3] Ahmed N, Talukdar S. Oscillatory MHD flow past a porous plate in a rotating system with periodic suction. Elixir Thermal Engg. 2011; 32: 2007-12.

[4] Mishra RB, Mishra P, Srivastava AK. A class of exact solutions of plane steady non-Newtonian MHD flow with variable viscosity. Elixir Appl. Math. 2011; 34: 2375-9.
[5] Baskaya S, Erturhan U, Sivrioglu M. Experimental investigation of mixed convection from an array, of discrete heat sources at the bottom of a horizontal channel. Heat Mass Transfer. 2005; 42: 56–63.
[6] Premachandran B, Balaji C. Mixed convection heat transfer from a horizontal channel with protruding heat sources. Heat Mass Transfer. 2005; 41: 510–18.
[7] Chamkha AJ, Ben-Naki A. MHD mixed convection–radiation interaction along a permeable surface immersed in a porous medium in the presence of Soret and Dufour effects. Heat Mass Trans. 2008; 44: 845–56.
[8] Murthy PVSN, Mukherjee S, Srinivasacharya D, Krishna PVSSSR. Combined radiation and mixed convection from a vertical wall with suction/injection in a non–Darcy porous medium. Acta Mechanica. 2004; 168: 145-56.
[9] Grosan T, Pop I. Thermal radiation effect on fully developed mixed convection flow in a vertical channel. Tech. Mech. 2007; 1: 37–47.
[10] Khaefinejad B, Aghanajafi C. Laminar flow with simultaneously effects of mixed convection and thermal radiation in a channel. J. Fusion Energy. 2009; 28: 83–90.
[11] Srinivas S, Muthuraj R. Effects of thermal radiation and space porosity on MHD mixed convection flow in a vertical channel using homotopy analysis method. Commun. Nonlinear Sci Numer Simulat. 2010; 15: 2098–108.
[12] Kafoussias NG, Williams EW. Thermal-diffusion and diffusion-thermo effects on mixed free-forced convective and mass transfer boundary layer flow with temperature dependent viscosity. Int. J. Eng. Sci. 1995; 33: 1369–84.
[13] Anghel M, Takhar HS, Pop I. Dufour and Soret effects on free-convection boundary layer over a vertical surface embedded in a porous medium. Studia Universitatis Babes-Bolyai, Mathematica. 2000; 45: 11–21.
[14] Postelnicu A. Influence of chemical reaction on heat and mass transfer by natural convection from vertical surfaces in porous media considering Soret and Dufour effects. Heat Mass Transfer. 2007; 43: 595–602.
[15] Kandasamy R, AnjaliDevi SP. Effects of chemical reaction, heat and mass transfer on non-linear laminar boundary later flow over a wedge with suction or injection. J. of Comp. and Appl. Mechanics. 2004; 5: 21–31.
[16] Kandasamy R, Periasamy K, Prabhu KKS. Effects of chemical reaction, heat and mass transfer along a wedge with heat source and concentration in the presence of suction or injection. Int. J. Heat Mass Transfer. 2005; 48: 1388–94.
[17] Seddeek MA. Finite-element method for the effects of chemical reaction, variable viscosity, thermophoresis and heat generation/absorption on a boundary-layer hydromagnetic flow with heat and mass transfer over a heat surface. Acta Mechanica. 2005; 177: 1–18.
[18] Mansour MA, El-Anssary NF, Aly AM. Effects of chemical reaction and thermal stratification on MHD free convective heat and mass transfer over a vertical stretching surface embedded in a porous media considering Soret and Dufour numbers. Chemical Engineering Journal. 2008; 145: 340–45.
[19] Joshi MY, Denn MM. Planar contraction flow with a slip boundary condition. J. Non-Newtonian Fluid Mech. 2003; 114: 185–95.
[20] Ebaid A. Effects of magnetic field and wall slip conditions on the peristaltic transport of a Newtonian fluid in an asymmetric channel. Physics Letters A. 2008; 372: 4493–9.
[21] Makinde OD, Chinyok T. MHD transient flows and heat transfer of dusty fluid in a channel with variable physical properties and Navier slip condition. Computers and Mathematics with Applications. 2010; 60: 660–9.
[22] RushiKumar B, Sivaraj R. Perturbation analysis of MHD mixed convective slip flow in a permeable vertical plate with Joule heating and soret effect. Elixir Appl. Math. 2011; 36: 3468-75.
[23] Cho K, Kim MU, Shin HD. Linear stability of two-dimensional steady flow in wavy-walled channels. Fluid Dynamics Res. 1998; 23: 349–70.
[24] Tashtoush B, Al-Odat M. Magnetic field effect on heat and fluid flow over a wavy surface with variable heat flux. J. Magn. Mater., 2004; 268: 357–63.
[25] Hady FM, Mohamed RA, Mahdy A. MHD free convection flow along a vertical wavy surface with heat generation or absorption effect. International Communications in Heat and Mass Transfer. 2006; 33: 1253–63.
[26] Muthuraj R, Srinivas S. Influence of magnetic field and wall slip conditions on steady flow between parallel flat wall and a long wavy wall with soret effect. Journal of Naval Architecture and Marine Engineering. 2009; 6: 62–71.
[27] Cogley AC, Vincent WG, Giles SE. Differential approximation to radiative heat transfer in a non-grey gas near equilibrium. A. I. A. A. J. 1968; 6: 551–3.

Appendix

$$I' = \int_0^\infty K_{\lambda w} \frac{\partial e_{b\lambda}}{\partial T} d\lambda \,;\; L_1 = \left[\frac{2-m_1}{m_1}\right] L \,;$$

$$R = V_0 d/\nu \,;\; M^2 = \sigma B_0^2 d^2/\mu \,;$$

$$Gr = g\beta_T\left(T_2 - T_1\right)d^3/\nu^2 \,; Gc = g\beta_C\left(C_2 - C_1\right)d^3/\nu^2$$

$$;\; Re = U_0 d/\nu \,;$$

$$Pr = \mu C_p / K \,;\; F = 4I'd^2/K \,;$$

$$\alpha_T = Q_T d^2 / K\left(T_2 - T_1\right); \alpha_C = Q_C d^2 / K\left(C_2 - C_1\right);$$

$$Df = D_m K_T\left(C_2 - C_1\right) / K C_S C_p\left(T_2 - T_1\right);$$

$$Pe = V_0 d / D_m \,;\; K_L = K_l d^2 / D_m \,;\; \gamma = L_1 / d \,;$$

$$h = 1 + \varepsilon\cos\lambda x \,;\; \varepsilon = \varepsilon^* / d \,;\; \lambda\ (= kd) \,;$$

$$A = dP/dX \,;$$

$$\beta_1 = \frac{-Pe + \sqrt{Pe^2 + 4K_L}}{2} \,; \quad \beta_2 = \frac{-Pe - \sqrt{Pe^2 + 4K_L}}{2} \,;$$

$$\beta_3 = \frac{-PrR + \sqrt{\left(PrR\right)^2 + 4\left(F + \alpha_T\right)^2}}{2} \,;$$

$$\beta_4 = \frac{-PrR - \sqrt{(PrR)^2 + 4(F+\alpha_T)^2}}{2};$$

$$\beta_5 = \frac{-R + \sqrt{R^2 + 4M^2}}{2};$$

$$\beta_6 = \frac{-R - \sqrt{R^2 + 4M^2}}{2}; \; A_1 = \frac{1}{(e^{\beta_1 h} - e^{\beta_2 h})};$$

$$A_2 = \frac{1}{(e^{\beta_2 h} - e^{\beta_1 h})}; \qquad A_3 = \frac{-A_1\left(\alpha_C + \beta_1^2 Df\right)}{\beta_1^2 + PrR\beta_1 - (F+\alpha_T)};$$

$$A_4 = \frac{-A_2\left(\alpha_C + \beta_2^2 Df\right)}{\beta_2^2 + PrR\beta_2 - (F+\alpha_T)};$$

$$A_5 = \frac{\left[1 + A_3\left(e^{\beta_4 h} - e^{\beta_1 h}\right) + A_4\left(e^{\beta_4 h} - e^{\beta_2 h}\right)\right]}{(e^{\beta_3 h} - e^{\beta_4 h})};$$

$$A_6 = \frac{\left[1 + A_3\left(e^{\beta_3 h} - e^{\beta_1 h}\right) + A_4\left(e^{\beta_3 h} - e^{\beta_2 h}\right)\right]}{(e^{\beta_4 h} - e^{\beta_3 h})};$$

$$A_7 = \frac{-\left(A_1 Gc + A_3 Gr\right)}{Re\left(\beta_1^2 + R\beta_1 - M^2\right)};$$

$$A_8 = \frac{-\left(A_2 Gc + A_4 Gr\right)}{Re\left(\beta_2^2 + R\beta_2 - M^2\right)};$$

$$A_9 = \frac{-A_5 Gr}{Re\left(\beta_3^2 + R\beta_3 - M^2\right)};$$

$$A_{10} = \frac{-A_6 Gr}{Re\left(\beta_4^2 + R\beta_4 - M^2\right)}; \; A_{11} = \frac{A}{M^2};$$

$$B_1 = A_7\begin{bmatrix}(1-\gamma\beta_1)(1+\gamma\beta_6)e^{\beta_6 h} - \\ (1+\gamma\beta_1)(1-\gamma\beta_6)e^{\beta_1 h}\end{bmatrix};$$

$$B_2 = A_8\begin{bmatrix}(1-\gamma\beta_2)(1+\gamma\beta_6)e^{\beta_6 h} - \\ (1+\gamma\beta_2)(1-\gamma\beta_6)e^{\beta_2 h}\end{bmatrix};$$

$$B_3 = A_9\begin{bmatrix}(1-\gamma\beta_3)(1+\gamma\beta_6)e^{\beta_6 h} - \\ (1+\gamma\beta_3)(1-\gamma\beta_6)e^{\beta_3 h}\end{bmatrix};$$

$$B_4 = A_{10}\begin{bmatrix}(1-\gamma\beta_4)(1+\gamma\beta_6)e^{\beta_6 h} - \\ (1+\gamma\beta_4)(1-\gamma\beta_6)e^{\beta_4 h}\end{bmatrix};$$

$$B_5 = A_{11}\left[(1+\gamma\beta_6)e^{\beta_6 h} - (1-\gamma\beta_6)\right];$$

$$B_6 = \begin{bmatrix}(1+\gamma\beta_5)(1-\gamma\beta_6)e^{\beta_5 h} - \\ (1-\gamma\beta_5)(1+\gamma\beta_6)e^{\beta_6 h}\end{bmatrix};$$

$$B_7 = A_7\begin{bmatrix}(1-\gamma\beta_1)(1+\gamma\beta_5)e^{\beta_5 h} - \\ (1+\gamma\beta_1)(1-\gamma\beta_5)e^{\beta_1 h}\end{bmatrix};$$

$$B_8 = A_8\begin{bmatrix}(1-\gamma\beta_2)(1+\gamma\beta_5)e^{\beta_5 h} - \\ (1+\gamma\beta_2)(1-\gamma\beta_5)e^{\beta_2 h}\end{bmatrix};$$

$$B_9 = A_9\begin{bmatrix}(1-\gamma\beta_3)(1+\gamma\beta_5)e^{\beta_5 h} - \\ (1+\gamma\beta_3)(1-\gamma\beta_5)e^{\beta_3 h}\end{bmatrix};$$

$$B_{10} = A_{10}\begin{bmatrix}(1-\gamma\beta_4)(1+\gamma\beta_5)e^{\beta_5 h} - \\ (1+\gamma\beta_4)(1-\gamma\beta_5)e^{\beta_4 h}\end{bmatrix};$$

$$B_{11} = A_{11}\left[(1+\gamma\beta_5)e^{\beta_5 h} - (1-\gamma\beta_5)\right];$$

$$B_{12} = \begin{bmatrix}(1+\gamma\beta_6)(1-\gamma\beta_5)e^{\beta_6 h} - \\ (1-\gamma\beta_6)(1+\gamma\beta_5)e^{\beta_5 h}\end{bmatrix};$$

$$A_{12} = \frac{(B_1 + B_2 + B_3 + B_4 + B_5)}{B_6};$$

$$A_{13} = \frac{(B_7 + B_8 + B_9 + B_{10} + B_{11})}{B_{12}}.$$

Table 1: Effect of F, α_T, α_C and Df in τ_0, τ_1, Nu_0 and Nu_1

Physical Parameters	Values	τ_0	τ_1	Nu_0	Nu_1
F	0.0	1.0451	4.3247	-1.1766	-0.6538
	0.5	1.0167	1.7259	-1.0844	-0.7912
	1.0	0.9907	-1.9816	-1.0008	-0.9221
α_T	1.0	1.0451	4.3247	-1.1766	-0.6538
	2.0	0.9907	-1.9816	-1.0008	-0.9221
	3.0	0.9448	-6.0126	-0.8558	-1.1668
α_C	0.0	0.8846	-8.6727	-0.6543	-1.4458
	1. 0	0.9376	-5.3272	-0.8276	-1.1839
	2.0	0.9907	-1.9816	-1.0008	-0.9221
Df	0.0	1.0381	-1.7240	-1.3260	-0.8726
	0.5	1.0144	-1.8528	-1.1634	-0.8973
	1.0	0.9907	-1.9816	-1.0008	-0.9221

Table 2: Effect of K_L, Pe and λ in τ_0, τ_1, Nu_0, Nu_1, Sh_0 and Sh_1

Physical Parameters	Values	τ_0	τ_1	Nu_0	Nu_1	Sh_0	Sh_1
K_L	0.0	0.9822	-5.6837	-0.8253	-1.1077	-1.5640	-0.5640
	0.5	0.9867	-4.4587	-0.9182	-1.0129	-1.4382	-0.7230
	1.0	0.9907	-1.9816	-1.0008	-0.9221	-1.3260	-0.8726
Pe	0.0	1.0048	11.7403	-1.3927	-0.6807	-0.8290	-1.2989
	0.5	0.9978	2.2985	-1.2143	-0.8170	-1.0590	-1.0675
	1.0	0.9907	-1.9816	-1.0008	-0.9221	-1.3260	-0.8726
λ	0.0	0.9907	-1.9816	-1.0008	-0.9221	-1.3260	-0.8726
	3.1	0.9732	-2.1365	-1.0392	-0.9607	-1.3738	-0.8994
	6.2	0.9907	-1.9816	-1.0008	-0.9221	-1.3260	-0.8726